Inorg. Chem. **2008**, *47*, 6771−6778

Kinetics and Mechanisms of the Oxidation of Iodide and Bromide in Aqueous Solutions by a *trans*-Dioxoruthenium(VI) Complex

William W. Y. Lam, Wai-Lun Man, Yi-Ning Wang, and Tai-Chu Lau*

Department of Biology and Chemistry, City University of Hong Kong, Tat Chee Avenue, Kowloon Tong, Hong Kong, China

Received February 28, 2008

The kinetics and mechanisms of the oxidation of I^- and Br^- by *trans*-$[Ru^{VI}(N_2O_2)(O)_2]^{2+}$ have been investigated in aqueous solutions. The reactions have the following stoichiometry: *trans*-$[Ru^{VI}(N_2O_2)(O)_2]^{2+} + 3X^- + 2H^+ \rightarrow$ *trans*-$[Ru^{IV}(N_2O_2)(O)(OH_2)]^{2+} + X_3^-$ (X = Br, I). In the oxidation of I^- the $I_3^-$is produced in two distinct phases. The first phase produces 45% of I_3^- with the rate law $d[I_3^-]/dt = (k_a + k_b[H^+])[Ru^{VI}][I^-]$. The remaining I_3^- is produced in the second phase which is much slower, and it follows first-order kinetics but the rate constant is independent of $[I^-]$, $[H^+]$, and ionic strength. In the proposed mechanism the first phase involves formation of a charge-transfer complex between Ru^{VI} and I^-, which then undergoes a parallel acid-catalyzed oxygen atom transfer to produce $[Ru^{IV}(N_2O_2)(O)(OHI)]^{2+}$, and a one electron transfer to give $[Ru^{V}(N_2O_2)(O)(OH)]^{2+}$ and $I^{\bullet}$. $[Ru^{V}(N_2O_2)(O)(OH)]^{2+}$ is a stronger oxidant than $[Ru^{VI}(N_2O_2)(O)_2]^{2+}$ and will rapidly oxidize another I^- to $I^{\bullet}$. In the second phase the $[Ru^{IV}(N_2O_2)(O)(OHI)]^{2+}$ undergoes rate-limiting aquation to produce HOI which reacts rapidly with I^- to produce I_2. In the oxidation of Br^- the rate law is $-d[Ru^{VI}]/dt = \{(k_{a2} + k_{b2}[H^+]) + (k_{a3} + k_{b3}[H^+])[Br^-]\}[Ru^{VI}][Br^-]$. At 298.0 K and $I = 0.1$ M, $k_{a2} = (2.03 \pm 0.03) \times 10^{-2}$ M^{-1} s^{-1}, $k_{b2} = (1.50 \pm 0.07) \times 10^{-1}$ M^{-2} s^{-1}, $k_{a3} = (7.22 \pm 2.19) \times 10^{-1}$ M^{-2} s^{-1} and $k_{b3} = (4.85 \pm 0.04) \times 10^{2}$ M^{-3} s^{-1}. The proposed mechanism involves initial oxygen atom transfer from *trans*-$[Ru^{VI}(N_2O_2)(O)_2]^{2+}$ to Br^- to give *trans*-$[Ru^{IV}(N_2O_2)(O)(OBr)]^{+}$, which then undergoes parallel aquation and oxidation of Br^-, and both reactions are acid-catalyzed.

Introduction

The oxidation of iodide to molecular iodine by one-electron oxidants has been extensively studied.[1] The oxidation of bromide to molecular bromine by a number of one-electron oxidants has also been reported. In oxidation by labile metal complexes, such as those of Mn(III),[2,3] Co(II),[4–7] V(V),[8] Rh(II),[9] and Ce(IV),[10] prior coordination of Br^- to the metal centers are involved. The intermediates then undergo either inter- or intramolecular (inner-sphere) oxidation of bromide. On the other hand, oxidation by substitution-inert metal complexes such as $[Ni(bipy)_3]^{3+}$ most likely occurs by outer-sphere electron-transfer.[11]

Oxidation of halides by metal peroxo species has also been extensively studied,[12–18] partly because of its relevance to the enzymes vanadium haloperoxidases, which catalyze the oxidation of halides by hydrogen peroxide, presumably via a vanadium peroxo intermediate.[19,20] These reactions involve oxygen atom transfer from the peroxo group to the halide.

* To whom correspondence should be addressed. E-mail: bhtclau@cityu.edu.hk.

(1) Nord, G. *Comments Inorg. Chem.* **1992**, *13*, 221–239.
(2) Wells, C. F.; Mays, D. *J. Chem. Soc. A.* **1968**, 577–583.
(3) Heyward, M. P.; Wells, C. F. *Inorg. Chim. Acta* **1988**, *148*, 241–246.
(4) Malik, M. N.; Hill, J.; McAuley, A. *J. Chem. Soc. A.* **1970**, 643–646.
(5) Davies, G.; Watkins, K. O. *J. Phys. Chem.* **1970**, *74*, 3388–3392.
(6) Bodek, I.; Davis, G.; Ferguson, J. H. *Inorg. Chem.* **1975**, *14*, 1708–1713.
(7) Rowan, N. S.; Price, C. Y.; Benjamin, W., III; Storm, C. B. *Inorg. Chem.* **1979**, *18*, 2044–2045.
(8) Julian, K.; Waters, W. A. *J. Chem. Soc.* **1962**, 818–821.
(9) Cannon, R. D.; Powell, D. B.; Sarawek, K. *Inorg. Chem.* **1981**, *20*, 1470–1474.
(10) Wells, C. F.; Nazer, A. F. M. *J. Chem. Soc., Faraday Trans. I.* **1979**, *75*, 816–824.
(11) Wells, C. F.; Fox, D. *J. Chem. Soc., Dalton Trans.* **1977**, 1502–1504.
(12) Clague, M. J.; Keder, N. L.; Butler, A. *Inorg. Chem.* **1993**, *32*, 4754–4761.
(13) Reynolds, M. S.; Morandi, S. J.; Raebiger, J. W.; Melican, S. P.; Smith, S. P. E. *Inorg. Chem.* **1994**, *33*, 4977–4984.
(14) Espenson, J. H.; Pestovsky, O.; Huston, P.; Staudt, S. *J. Am. Chem. Soc.* **1994**, *116*, 2869–2877.
(15) Clague, M. J.; Butler, A. *J. Am. Chem. Soc.* **1995**, *117*, 3475–3484.
(16) Colpas, G. J.; Hamstra, B. J.; Kampf, J. W.; Pecoraro, V. L. *J. Am. Chem. Soc.* **1996**, *118*, 3469–3478.
(17) Reynolds, M. S.; Babinski, J. K.; Bouteneff, M. C.; Brown, J. L.; Campbell, R. E.; Cowan, M. A.; Durwin, M. R.; Foss, T.; O'Brien, P.; Penn, H. R. *Inorg. Chim. Acta* **1997**, *263*, 225–230.
(18) Lemma, K.; Bakac, A. *Inorg. Chem.* **2004**, *43*, 4505–4510.

10.1021/ic8003849 CCC: $40.75
Published on Web 07/02/2008

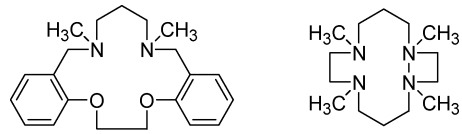

Figure 1. Structures of N_2O_2 and tmc.

The oxidation of halides by metal-oxo species is also of interest, partly because of its relevance to heme chloroperoxidases (CPO), which catalyze the oxidative halogenation of substrates using H_2O_2 and halide. CPO is a heme-containing enzyme, and the active intermediate is believed to be similar to that in cytochrome P450, that is, $Fe^{IV}=O(P^{+\bullet})$.[21] There are, however, only a few reports on the oxidation of halides by metal-oxo species. In the oxidation of I^- and Br^- by MnO_4^- two-electron mechanisms were proposed.[22–24] Oxidation of Br^- by an oxomanganese(V) porphyrin species proceeds by reversible oxygen atom transfer.[25] On the other hand, a one-electron mechanism was proposed in oxidation by $Cr_{aq}O^{2+}$.[26]

We have previously reported the kinetics and mechanism of the oxidation of I^- by *trans*-$[Ru^{VI}(tmc)(O)_2]^{2+}$ (tmc = 1,4,8,11-tetramethyl-1,4,8,11-tetraazacyclotetradecane, Figure 1).[27] The proposed mechanism involves initial reversible oxygen atom transfer from Ru^{VI} to I^-, followed by rate-limiting acid-catalyzed aquation of the resulting $Ru^{IV}-OI$ species to give HOI, which then rapidly oxidizes I^- to I_2. The UV/vis spectral changes reveal only one step with a well-defined isosbestic point, suggesting that the intermediates are present in very low concentrations. In this paper we report the kinetics of the oxidation of I^- in aqueous solution by a more strongly oxidizing *trans*-dioxoruthenium(VI) complex, *trans*-$[Ru^{VI}(N_2O_2)(O)_2]^{2+}$ (N_2O_2 = 1,12-dimethyl-3,4,:9,10-dibenzo-1.12-diaza-5,8-dioxacyclopentadecane, Figure 1). We hoped that in this system the equilibrium concentration of $[O{=}Ru^{IV}-OI]^+$ or HOI, if formed, would be high enough to be detected. We also report the kinetics of the oxidation of Br^- by this complex, which in contrast to *trans*-$[Ru^{VI}(tmc)(O)_2]^{2+}$, is thermodynamically capable of oxidizing Br^-. The oxidation of various substrates by *trans*-$[Ru^{VI}(N_2O_2)(O)_2]^{2+}$ has been reported.[28–33] Thermodynamic data (E^0 vs NHE and pK_a values, 298 K) for the *trans*-$[Ru^{VI}(N_2O_2)(O)_2]^{2+}$ system are summarized in Scheme 1.[28,33]

Experimental Section

Materials. *trans*-$[Ru^{VI}(N_2O_2)(O)_2](ClO_4)_2$ was prepared according to a literature method.[28] Potassium iodide was obtained from BDH (AR grade) and was used as received. Potassium bromide (Aldrich) was recrystallized from water.[34] Water for kinetic measurements was distilled twice from alkaline permanganate. The pH of the solutions were maintained with either CF_3CO_2H or phosphate buffer, and the ionic strength were adjusted using CF_3CO_2Na. D_2O (99.9 atom% D) was obtained from Aldrich. The pD values for D_2O solutions were determined by using a pH meter (Delta 320) using the relationship $pD = pH_{meas} + 0.4$.

Kinetics. The kinetics of the reactions were studied by using either an Applied Photophysics SX20 stopped-flow spectrophotometer or a Hewlett-Packard 8452A diode-array spectrophotometer. The concentrations of I^- or Br^- were at least in 10-fold excess of that of Ru^{VI}. The reaction progress was monitored by observing the absorbance changes at either 353 nm (λ_{max} of I_3^-) for I^- or 266 nm (λ_{max} of Br_3^-) for Br^-. Solutions of I^- and Br^- were freshly prepared using deaerated water. Pseudo-first-order rate constants, k_{obs}, were obtained by nonlinear least-squares fits of A_t versus time t according to the equation $A_t = A_\infty + (A_0 - A_\infty)\exp(-k_{obs}t)$, where A_0 and A_∞ are the initial and final absorbance, respectively. Activation parameters were obtained from plots of $\ln(k/T)$ versus $1/T$ according to the Eyring equation.

Mass spectrometry. Electrospray ionization mass spectrometry (ESI/MS) was done on a PE SCIEX API 365 triple quadruple mass spectrometer. The analyte solution was continuously infused with a syringe pump at a constant flow rate of 5 μL min^{-1} into the pneumatically assisted electrospray probe with nitrogen as the nebulizing gas. The declustering potential was typically set at 10−20 V.

Product Analysis. In the oxidation of I^- the amount of I_3^- produced was determined spectrophotometrically at 353 nm by using the known value of ε (2.6×10^4 M^{-1} cm^{-1}) for I_3^- and the equilibrium constant for the following reaction: $I^- + I_2 \rightleftharpoons I_3^-$ (K = 721 M^{-1}).[35] In the oxidation of Br^- the Br_2 product was detected by extracting the solution after reaction ($[Ru^{VI}] = 2 \times 10^{-4}$ M and $[Br^-] = 4 \times 10^{-4}$ M in $[H^+] = I = 0.1$ M) with CCl_4 and then shaking with aqueous sodium iodide. The color of the CCl_4 layer changed to pink, indicating the presence of Br_2.[36] In a separate experiment, a solution of Ru^{VI} (1×10^{-4} M) was allowed to react with excess Br^- (0.1 M) in 0.01 M H^+. Repetitive scanning of the UV/vis absorption spectra of the solution showed increase in absorbance at 266 nm, consistent with the formation of Br_3^-. The solution after reaction was then passed through a Sephadex-SP C-25 cation-exchange column. On examination of the UV/vis spectrum of the effluent solution, $(1.1 \pm 0.1) \times 10^{-4}$ M of Br_3^- was found to be produced, that is, one mole of Br_2 was produced per mole of Ru^{VI}. The following data were used in calculating $[Br_3^-]$; K = 16.1 for the equilibrium $Br^- + Br_2 \rightleftharpoons Br_3^-$ and $\varepsilon_{266nm} = 4.1 \times 10^4$ M^{-1} cm^{-1} for Br_3^-.[37] Chromatography is necessary prior to the analysis

(19) Slebodnick, C., Law, N. A., Pecoraro, V. L., In *Biomimetic Oxidations Catalyzed by Transition Metal Complexes*; Meunier, B., Ed.; Imperial College Press: London, 2000; pp 215−267.
(20) Butler, A. *Coord. Chem. Rev.* **1999**, *187*, 17–35.
(21) Meunier, B. In *Biomimetic Oxidations Catalyzed by Transition Metal Complexes*; Meunier, B., Ed.; Imperial College Press: London, 2000; pp 171−214.
(22) Kirschenbaum, J.; Sutter, J. R. *J. Phys. Chem.* **1966**, *70*, 3863–3866.
(23) Lawani, S. A.; Sutter, J. R. *J. Phys. Chem.* **1973**, *77*, 1547–1551.
(24) Lawani, S. A. *J. Phys. Chem.* **1976**, *80*, 105–107.
(25) Jin, N.; Bourassa, J. L.; Tizio, S. C.; Groves, J. T. *Angew. Chem., Int. Ed.* **2000**, *39*, 3849–3851.
(26) Hung, M.; Bakac, A. *Inorg. Chem.* **2005**, *44*, 9293–9298.
(27) Lau, T. C.; Lau, K. W. C.; Lau, K. *J. Chem. Soc., Dalton Trans.* **1994**, 3091–3093.
(28) Che, C. M.; Tang, W. T.; Wong, W. T.; Lai, T. F. *J. Am. Chem. Soc.* **1989**, *111*, 9048–9056.
(29) Che, C. M.; Tang, W. T.; Lee, W. O.; Wong, K. Y.; Lau, T. C. *J. Chem. Soc., Dalton Trans.* **1992**, 1551–1556.
(30) Yiu, D. T. Y.; Chow, K. H.; Lau, T. C. *J. Chem. Soc., Dalton Trans.* **2000**, 17–20.
(31) Yiu, D. T. Y.; Lee, M. F. W.; Lam, W. W. Y.; Lau, T. C. *Inorg. Chem.* **2003**, *42*, 1225–1232.
(32) Lam, W. W. Y.; Yiu, S. M.; Yiu, D. T. Y.; Lau, T. C.; Yip, W. P.; Che, C. M. *Inorg. Chem.* **2003**, *42*, 8011–8018.
(33) Man, W. L.; Lam, W. W. Y.; Wong, W. Y.; Lau, T. C. *J. Am. Chem. Soc.* **2006**, *128*, 14669–14675.
(34) Armarego, W. L. F.; Perrin, D. D. *Purification of Laboratory Chemicals*, 4th ed.; Reed Educational and Professional Publishing Ltd: Oxford, 1996.
(35) Troy, R. C.; Kelley, M. D.; Nagy, J. C.; Margerum, D. W. *Inorg. Chem.* **1991**, *30*, 4838–4845.
(36) Birk, J. P. *Inorg. Chem.* **1978**, *17*, 504–506.

Scheme 1. Thermodynamic Data for the *trans*-$[Ru^{VI}(N_2O_2)(O)_2]^{2+}$ System

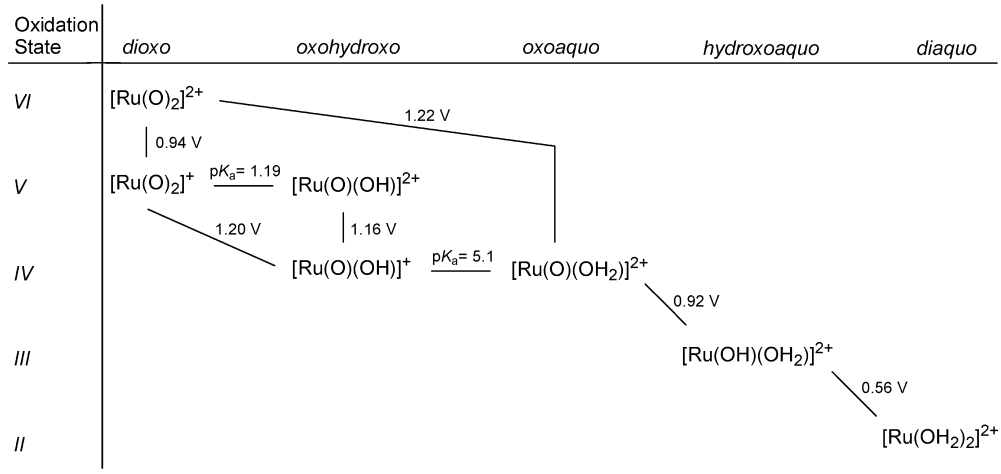

of Br_3^- because the cationic ruthenium product has substantial absorption at 266 nm.

The ruthenium product was determined as follows. A solution of Ru^{VI} (1×10^{-4} M) was allowed to react with excess Br^- or I^- (4×10^{-3} M) in 0.01 M H^+ at 298.0 K. The resulting solution was loaded onto a Sephadex-SP C-25 cation-exchange column and then eluted with 0.2 M $HClO_4$. Examination of the UV/vis spectrum of the eluted solution indicated almost quantitative formation [$(0.9 \pm 0.1) \times 10^{-4}$ M] of *trans*-$[Ru^{IV}(N_2O_2)(O)(OH_2)]^{2+}$ [λ_{max}/nm (ε/dm^3 mol^{-1} cm^{-1}): 540(120), 265(2400), 232(8300)].[28]

Results and Discussion

Oxidation of Iodide. Spectral Changes and Stoichiometry. Rapid formation of I_3^- (λ_{max} at 288 and 352 nm) was observed when a solution of *trans*-$[Ru^{VI}(N_2O_2)(O)_2]^{2+}$ (8×10^{-5} M) was mixed with a solution of I^- (1×10^{-3} M) at 298.0 K, pH = 3.01, and $I = 0.1$ M (Figure 2). The final spectrum (after ca. 500 s) indicated the formation of one mol equivalent of I_3^- (7.8×10^{-5} M). $[Ru^{IV}(N_2O_2)(O)(OH_2)]^{2+}$ was also produced quantitatively (see Experimental Section).

These results suggest the overall stoichiometry shown in eqs 1 and 2.[38]

$$\textit{trans}\text{-}[Ru^{VI}(N_2O_2)(O)_2]^{2+} + 2I^- + 2H^+ \rightarrow \textit{trans}\text{-}[Ru^{IV}(N_2O_2)(O)(OH_2)]^{2+} + I_2 \quad (1)$$

$$I^- + I_2 \overset{K}{\rightleftharpoons} I_3^- \quad (2)$$

On the basis of the E^0 for $[Ru^{VI}(N_2O_2)(O)_2]^{2+}/[Ru^{IV}(N_2O_2)(O)(OH_2)]^{2+}$ (1.22 V) and I_2/I^- (0.54 V), E^0 for the reaction shown in eq 1 is 0.68 V.

Repetitive scanning using a combination of stopped-flow and convention UV−vis diode array spectrophotometers (Figure 2) indicates that the formation of I_3^- occurs in two distinct phases. The first phase results in the formation of about 45% of I_3^- while the remaining I_3^- is formed in a second phase which is much slower.

Kinetics. The kinetics of the first phase were studied at pH 3−5.3 (Supporting Information, Table S1), at lower pH the reaction was too fast to be followed even by stopped-flow methods. Clean pseudo-first-order kinetics were observed in the presence of at least 10-fold excess of I^- (Figure

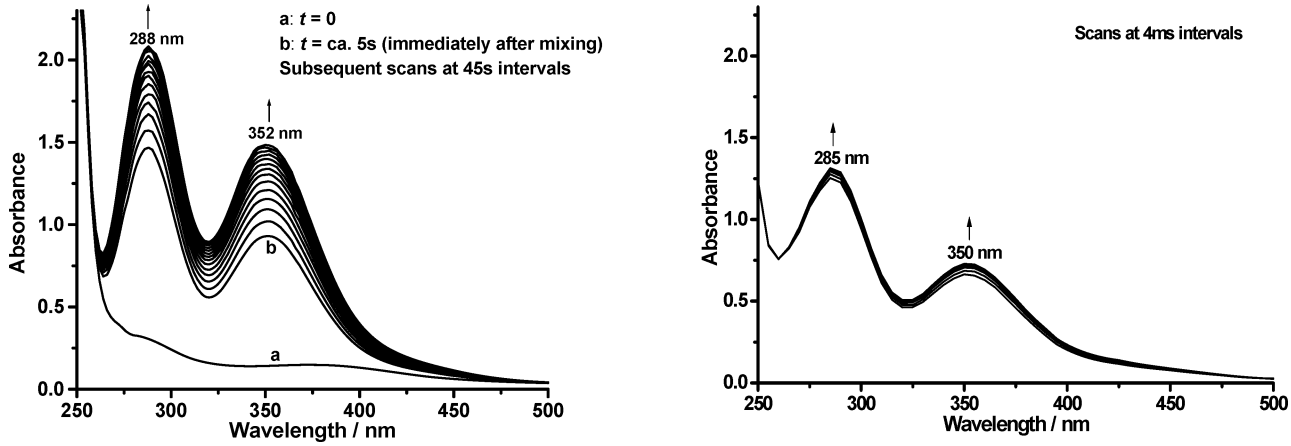

Figure 2. Spectral changes for the oxidation of I^- (1×10^{-3} M) by *trans*-$[Ru^{VI}(N_2O_2)(O)_2]^{2+}$ (8×10^{-5} M) at 298.0 K, pH = 3.01, and $I = 0.1$ M. Left panel: spectra obtained with a diode-array spectrophotometer using a two-compartment cuvette. Right panel: spectra obtained with a stopped-flow spectrophotometer using point by point method.

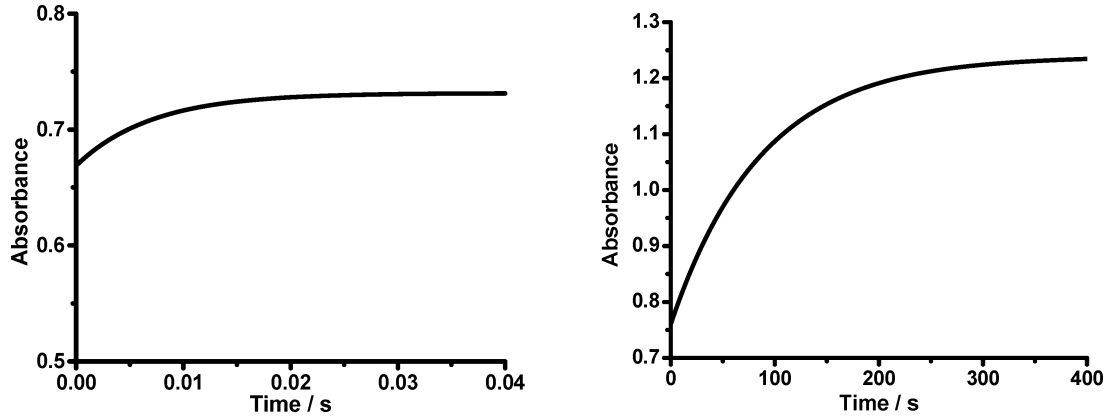

Figure 3. Left panel: Absorbance-time trace at 353 nm for the first phase of the oxidation of I^- (1×10^{-3} M) by *trans*-$[Ru^{VI}(N_2O_2)(O)_2]^{2+}$ (1×10^{-4} M) at 298.0 K, pH = 3.01, and $I = 0.1$ M. Right panel: Absorbance-time trace at 352 nm for the second phase of the reaction.

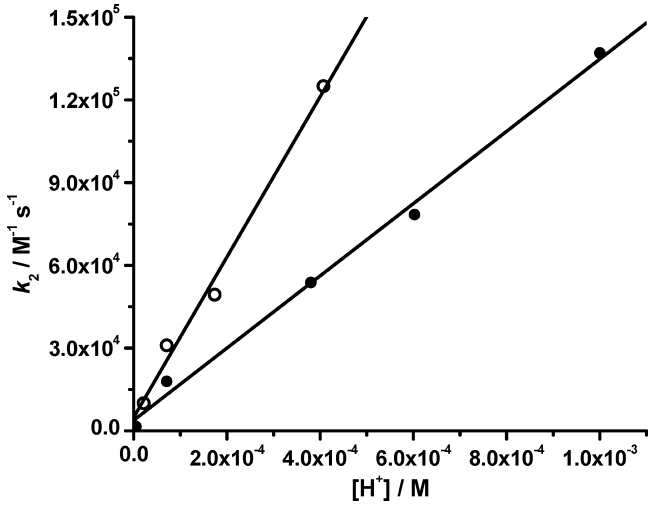

Figure 4. Plot of k_2 vs $[H^+]$ (solid circle) and $[D^+]$ (open circle) for the first phase of the oxidation of I^- by *trans*-$[Ru^{VI}(N_2O_2)(O)_2]^{2+}$ at 298.0 K and $I = 0.1$ M [For solid circle: slope = $(1.31 \pm 0.05) \times 10^8$; *y*-intercept = $(3.83 \pm 2.89) \times 10^3$; $r = 0.998$. For open circle: slope = $(2.91 \pm 0.20) \times 10^8$; *y*-intercept = $(4.92 \pm 4.50) \times 10^3$; $r = 0.995$].

3). The pseudo-first-order rate constants, k_{obs}, are independent of $[Ru^{VI}]$ ($5 \times 10^{-5}-2 \times 10^{-4}$ M) but depend linearly on $[I^-]$ ($1 \times 10^{-3}-4 \times 10^{-3}$ M). The rate of reaction is also increased by an increase in $[H^+]$; the plot of k_2, the second order rate constant, versus $[H^+]$ is linear with a relatively small intercept (Figure 4). These results are consistent with the rate law shown in eq 3.

$$d[I_3^-]/dt = (k_a + k_b[H^+])[Ru^{VI}][I^-] \quad (3)$$

At 298.0 K and $I = 0.1$ M, k_a and k_b are $(3.8 \pm 2.9) \times 10^3$ M^{-1} s^{-1} and $(1.31 \pm 0.05) \times 10^8$ M^{-2} s^{-1}, respectively. At low pH (1−4) the acid-independent pathway (k_a) is insignificant. At pH = 3.01 and $I = 0.1$ M, $\Delta H^{\ddagger}$ and $\Delta S^{\ddagger}$ are (7.6 ± 0.4) kcal mol^{-1} and $-(9 \pm 2)$ cal mol^{-1} K^{-1}, respectively (Supporting Information, Figure S1).

The kinetics were also studied in D_2O at $I = 0.1$ M and 298.0 K (Figure 4). $k_a(D_2O)$ and $k_b(D_2O)$ were $(4.92 \pm 4.50) \times 10^3$ M^{-1} s^{-1} and $(2.91 \pm 0.20) \times 10^8$ M^{-2} s^{-1}, respectively; this gives $k_b(H_2O)/k_b(D_2O) = 0.45 \pm 0.05$.

The second phase of the reaction also follows clean pseudo-first-order kinetics; however, the pseudofirst-order rate constant is independent of $[I^-]$ and $[Ru^{VI}]$ ($[I^-] = 1 \times$

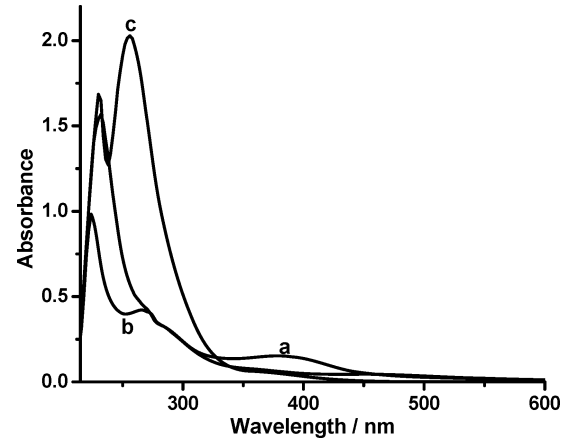

Figure 5. (a) Spectrum of I^- (7×10^{-5} M) and *trans*-$[Ru^{VI}(N_2O_2)(O)_2]^{2+}$ (8×10^{-5} M) in 0.1 M CF_3CO_2H in a two-compartment cuvette before mixing; (b) spectrum ~5 s after mixing; (c) spectrum after addition of 1 M Br^- (λ_{max} at 254 nm).

$10^{-4}-1 \times 10^{-2}$ M, $[Ru^{VI}] = 1 \times 10^{-5}-1 \times 10^{-4}$ M). The reaction is also independent of pH; at pH = 1.0 and $I = 0.1$ M, $k = (1.33 \pm 0.05) \times 10^{-2}$ s^{-1}; at pH = 4.36, $I = 0.1$ M, $k = (1.43 \pm 0.16) \times 10^{-2}$ s^{-1} (Supporting Information, Table S3).

Detection of the Intermediate. A solution of Ru^{VI} (8×10^{-5} M) was allowed to react with slightly less than 1 equiv of I^- (7×10^{-5} M) at 298.0 K and $[H^+] = 0.1$ M. After about 30 s, excess Br^- (1 M) was added, and the UV/vis spectrum shows the formation of a species that absorbs at 254 nm, suggesting that it is IBr_2^- ($\lambda_{max} = 253$ nm, $\varepsilon = 55\,000$ M^{-1} cm^{-1})[35] (Figure 5). The presence of IBr_2^- was also detected by ESI/MS. The ESI mass spectrum (Figure 6) of a similar reaction mixture[39] in the negative mode shows a peak at $m/z = 287$ which is assigned to IBr_2^-; MS/MS of this peak produces Br^- ($m/z = 80$).[40] (If Ru^{VI} was allowed to react with excess I^- without adding Br^-, then the ESI mass spectrum shows the presence of I_3^-, as expected). These results suggest the presence of either free or coordinated HOI

(37) Wang, T. X.; Kelley, M. D.; Cooper, J. N.; Beckwith, R. C.; Margerum, D. W. *Inorg. Chem.* **1994**, *33*, 5872–5878.
(38) There is a further much slower reaction, presumably due to further reduction of $[Ru^{IV}(N_2O_2)(O)(OH_2)]^{2+}$ by I^-. Also at higher $[I^-]$ it is possible that $[Ru^{IV}(N_2O_2)(O)(I)]^+$ is formed.
(39) An equal volume of CH_3CN was added to the sample solution before electrospraying to increase the sensitivity of the MS signal.

in solution, which would react with Br^- to form IBr_2^- according to eqs 4 and 5.[35] (HOI has a relatively low absorption in the UV/vis region,[41] so it would not be detected spectrophotometrically unless converted to a highly absorbing species such as IBr_2^-. Also the neutral HOI should not be observed by ESI/MS.) From the absorbance at 254 nm (A_{254} = 2.0), $[IBr_2^-]$ is calculated to be 3.6×10^{-5} M, which is around 50% yield (based on I^-). Some HOI may have undergone disproportionation, which is known to be rapid.[42]

$$HOI + H^+ + Br^- \rightleftharpoons IBr + H_2O \qquad K = 4.2 \times 10^6\ M^{-2} \tag{4}$$

$$IBr + Br^- \rightleftharpoons IBr_2^- \qquad K = 286\ M^{-1} \tag{5}$$

Mechanism. The proposed mechanism is represented by eqs 6–13

Phase I

$$[O{=}Ru^{VI}{=}O]^{2+} + I^- + H^+ \overset{K_{CT}}{\rightleftharpoons} \{[O{=}Ru^{VI}{=}O]^{2+}, I^-, H^+\} \tag{6}$$

$$\{[O{=}Ru^{VI}{=}O]^{2+}, I^-, H^+\} \xrightarrow{k_7} [O{=}Ru^{IV}{-}OHI]^{2+} \tag{7}$$

$$\{[O{=}Ru^{VI}{=}O]^{2+}, I^-, H^+\} \xrightarrow{k_8} [O{=}Ru^{V}{-}OH]^{2+} + I^\bullet \tag{8}$$

$$[O{=}Ru^{V}{-}OH]^{2+} + I^- \rightarrow [O{=}Ru^{IV}{-}OH]^{+} + I^\bullet \tag{9}$$

$$2I^\bullet \rightarrow I_2 \tag{10}$$

$$[O{=}Ru^{IV}{-}OH]^{+} + H^+ \rightarrow [O{=}Ru^{IV}{-}OH_2]^{2+} \tag{11}$$

Phase II

$$[O{=}Ru^{IV}{-}OHI]^{2+} + H_2O \xrightarrow{\text{slow}} [O{=}Ru^{IV}{-}OH_2]^{2+} + HOI \tag{12}$$

$$HOI + H^+ + I^- \xrightarrow{\text{fast}} H_2O + I_2$$

$$(k_{13} = 4.4 \times 10^{12}\ M^{-2}\ s^{-1})^{43} \tag{13}$$

The reduction of $[Ru^{VI}(N_2O_2)(O)_2]^{2+}$ to $[Ru^{IV}(N_2O_2)(O)(OH_2)]^{2+}$ by excess I^- in aqueous acidic solutions results in the quantitative formation of I_3^-. However, I_3^- is produced in two distinct phases. The first phase has only a relatively small absorbance change ($\sim$ 0.68−0.73 at 353 nm), but the spectrum after $\sim$30 ms indicates the formation of 45% I_3^-. The second phase produces the remaining 55% I_3^-, but it has a much larger absorbance change ($\sim$ 0.75−1.25). Our only explanation is that a hydrogen-bonded Ru^{VI} and I^- first form a charge-transfer complex (eq 6 and Scheme 2) that has a similar absorption spectrum to that of I_3^-, so that its subsequent conversion to I_3^- would produce a small spectral change.

The proposed subsequent reactions of this charge-transfer complex are as follow. This species undergoes parallel acid-catalyzed oxygen atom transfer (OAT) to produce $[Ru^{IV}(N_2O_2)(O)(OHI)]^{2+}$ (eq 7) and one-electron transfer (ET) to give $[Ru^{V}(N_2O_2)(O)(OH)]^{2+}$ and $I^\bullet$ (eq 8). $[Ru^{V}(N_2O_2)(O)(OH)]^{2+}$ is a stronger oxidant than $[Ru^{VI}(N_2O_2)(O)_2]^{2+}$ and will rapidly oxidize another I^- to $I^\bullet$ (eq 9). Equations 6–10 account for the observed rate law (neglecting the acid-independent pathway) given in eq 3 with $k_b = K_{CT}k_8$. The OAT pathway is supported by the observation of IBr_2^- upon adding excess Br^- to a reaction mixture of Ru^{VI} and $\sim$0.9 mol equivalent of I^-. IBr_2^- would be formed from the reaction of Br^- with $[Ru^{IV}(N_2O_2)(O)(OHI)]^{2+}$. From the E^0 values given in eqs 14 and 15, the OAT step should be downhill. Also from the E^0 for the $I^\bullet/I^-$ couple of 1.33 V[44] and the E^0 for $[Ru^{VI}(N_2O_2)(O)_2]^{2+}/[Ru^{V}(N_2O_2)(O)_2]^{+}$ couple of 0.94 V, ΔG^0 for the one-electron transfer pathway is 8.9 kcal mol^{-1}, which is lower than the observed $\Delta G^\ddagger$ value of 10.2 ± 0.5 kcal $mo1^{-1}$ at pH = 3, so this pathway is possible.

$$O{=}Ru^{VI}{=}O + 2H^+ + 2e^- \rightarrow O{=}Ru^{IV}{-}OH_2 \qquad E^0 = 1.22\ V \tag{14}$$

$$HOI + H^+ + 2e^- \rightarrow I^- + H_2O \qquad E^0 = 1.0\ V \tag{15}$$

The acid catalysis observed in the OAT and ET steps could be due to a pre-equilibrium step involving protonation of an oxo ligand of $[Ru^{VI}(N_2O_2)(O)_2]^{2+}$; however this is probably not the case, since there is no evidence for protonation of the Ru^{VI} species even in 6 M H^+. Moreover the rates of oxidation of other substrates such as $[Ru(NH_3)_4(isn)_2]^{2+}$ (isn = isonicotinamide) are independent of pH (from 1−3).[45] Instead, the acid-catalyzed OAT and ET pathways could occur by proton-assisted oxygen atom transfer, that is, the I^- could combine with a hydrogen-bonded Ru^{VI} complex (Scheme 2).

The rate of formation of the remaining 55% of I_3^- in the second phase of the reaction is independent of $[I^-]$, $[H^+]$, and ionic strength. We propose that this phase involves initial rate-limiting aquation of $[O{=}Ru^{IV}{-}OHI]^{2+}$ to give $[O{=}Ru^{IV}{-}OH_2]^{2+}$ (eq. 12), followed by rapid reaction between HOI and I^- to give I_2 (eq 13).[44] The observed 50% yield of HOI is in reasonable agreement with the observed 55% yield of I_3^-, given the fact that HOI is a rather unstable species. This proposed mechanism implies that the coordinated HOI reacts more slowly with I^- than free HOI, which is not unreasonable since the bulky macrocyclic ligand N_2O_2 could impose substantial steric effects on the approach of I^-.

(40) (a) The ESI/MS of polyhalide ions have been reported: McIndoe, J. S.; Tuck, D. G. *J. Chem. Soc., Dalton Trans.* **2003**, 244–248. (b) Crawford, E.; McIndoe, J. S.; Tuck, D. G. *Can. J. Chem.* **2006**, *84*, 1607–1613.
(41) Bichel, Y.; Gunten, U. R. *Water Res.* **2000**, *34*, 3197–3203.
(42) Urbansky, E. T.; Cooper, B. T.; Margerum, D. W. *Inorg. Chem.* **1997**, *36*, 1338–1344.
(43) Eigen, M.; Kustin, K. *J. Am. Chem. Soc.* **1962**, *84*, 1355–1361.
(44) Stanbury, D. M.; Wilmarth, W. K.; Khalaf, S.; Po, H. N.; Byrd, J. E. *Inorg. Chem.* **1980**, *19*, 2715–2722.
(45) Li, C. K. PhD Thesis, University of Hong Kong, 1991.

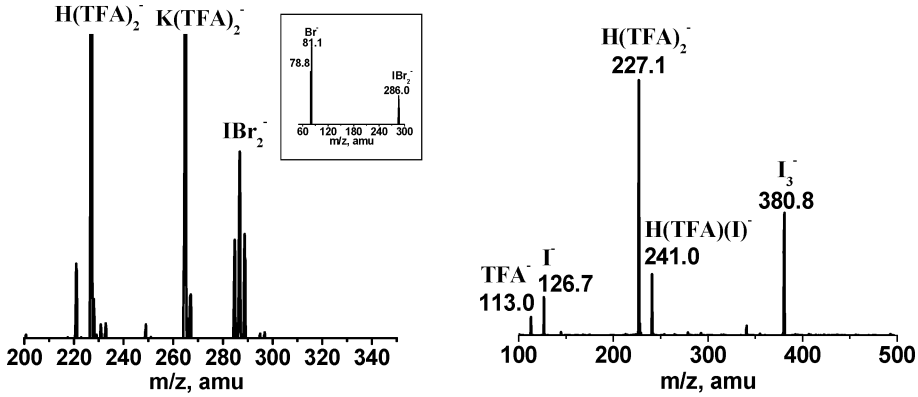

Figure 6. Left panel: ESI/MS (-ve mode) of the solution produced by adding KBr (0.01 M) to a reaction mixture of $[Ru^{VI}(N_2O_2)(O)_2](ClO_4)_2$ (7×10^{-4} M) and KI (6×10^{-4} M) in 0.1 M CF_3CO_2H. Insets shows MS/MS of the ion at $m/z = 286$. Right panel: ESI-MS (-ve mode) of solution containing $[Ru^{VI}(N_2O_2)(O)_2](ClO_4)_2$ (5×10^{-4} M) + KI (0.05 M) in 0.1 M CF_3COOH.

Scheme 2. Proton-Assisted Oxygen Atom Transfer and Electron Transfer

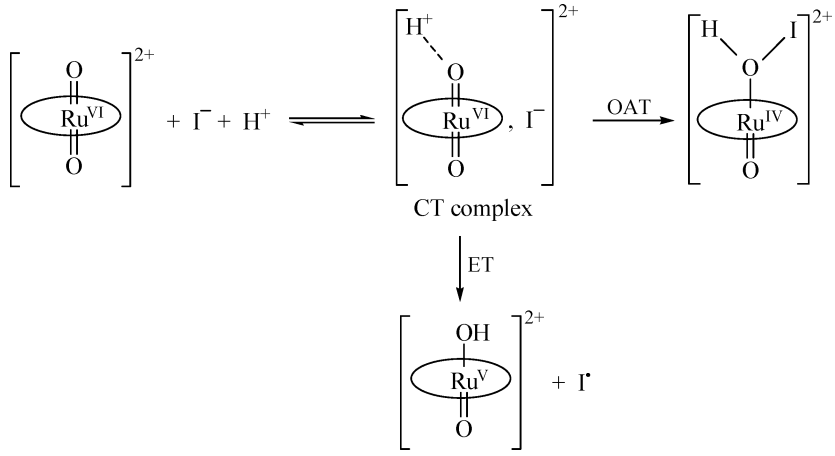

Oxidation of Bromide. Spectral Changes. Figure 7 shows the spectral changes when a solution of Br^- (1×10^{-2} M) was mixed with a solution of Ru^{VI} (1×10^{-4} M) at $[H^+] = 0.07$ M and $I = 0.1$ M. In contrast to the oxidation of I^-, only one phase was observed in this case, with well-defined isosbestic points at 260 and 315 nm that were maintained throughout the reaction. The increase in absorbance at 266 nm is consistent with the formation of Br_3^-. Analysis by UV−vis spectrophotometry (after passing the solution through a cation-exchange column) showed that 1 mol of Br_3^- is produced per mol of Ru^{VI}. Br_2 was also

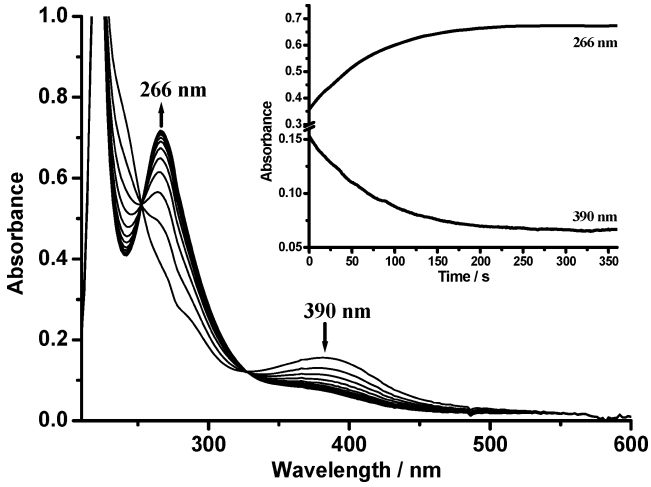

Figure 7. Spectral changes at 30 s intervals for the reaction of Br^- (1×10^{-2} M) with *trans*-$[Ru^{VI}(N_2O_2)(O)_2]^{2+}$ (1×10^{-4} M) at 298.0 K, $[H^+] = 0.07$ M, and $I = 0.1$ M. Inset shows the corresponding kinetic traces at 266 and 390 nm.

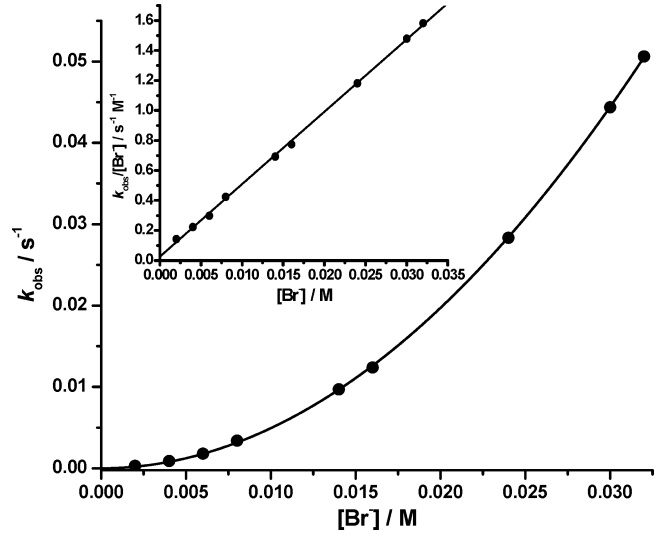

Figure 8. Plot of k_{obs} vs $[Br^-]$ for the oxidation of Br^- by *trans*-$[Ru^{VI}(N_2O_2)(O)_2]^{2+}$ at 298.0 K, $[H^+]$ and $I = 0.1$ M. Inset shows the corresponding plot of $k_{obs}/[Br^-]$ vs $[Br^-]$ [slope = $(4.82 \pm 0.02) \times 10^1$; y-intercept = $(3.43 \pm 0.26) \times 10^{-2}$; $r = 0.9996$].

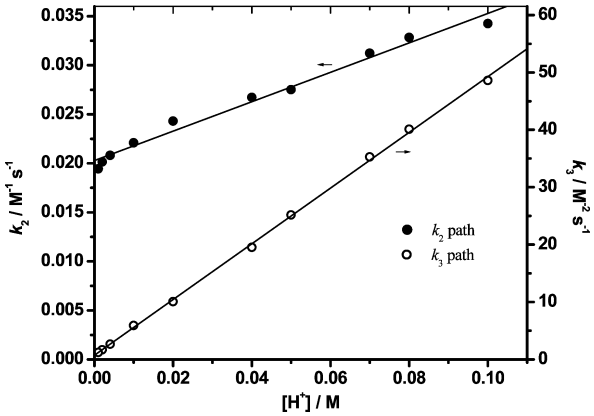

Figure 9. Plots of k_2 and k_3 vs $[H^+]$ for the oxidation of Br^- by *trans*-$[Ru^{VI}(N_2O_2)(O)_2]^{2+}$ at 298.0 K and $I = 0.1$ M [For k_2 path: slope = (1.50 ± 0.07) × 10^{-1}; *y*-intercept = (2.03 ± 0.03) × 10^{-2}; $r = 0.9922$. For k_3 path: slope = (4.85 ± 0.04) × 10^2; *y*-intercept = (7.22 ± 2.19) × 10^{-1}; $r = 0.9997$].

detected by extracting the solution after reaction with CCl_4 and treating with aqueous NaI (see Experimental Section). Hence, the reaction can be represented by eqs 16 and 17.

$$\textit{trans}\text{-}[Ru^{VI}(N_2O_2)(O)_2]^{2+} + 2Br^- + 2H^+ \rightarrow \textit{trans}\text{-}[Ru^{IV}(N_2O_2)(O)(OH_2)]^{2+} + Br_2 \quad (16)$$

$$Br^- + Br_2 \overset{K}{\rightleftharpoons} Br_3^- \quad (17)$$

On the basis of the E^0 for $[Ru^{VI}(N_2O_2)(O)_2]^{2+}/[Ru^{IV}(N_2O_2)(O)(OH_2)]^{2+}$ (1.22 V) and Br_2/Br^- (1.09 V),[46] E^0 for the reaction shown in eq 16 is 0.13 V.

Kinetics. The kinetics of the reaction were monitored at either 266 or 390 nm. The rate constants obtained at both wavelengths are the same. Clean pseudo-first-order kinetics were observed for over three half-lives in the presence of at least 10-fold excess of Br^-. The pseudo-first-order rate constants, k_{obs}, are independent of $[Ru^{VI}]$ (5×10^{-5}–2×10^{-4} M) but increase with $[Br^-]$ (1×10^{-3}–3×10^{-2} M) (Figure 8). The plot of $k_{obs}/[Br^-]$ versus $[Br^-]$ is linear (Figure 8), indicating the following relationship:

$$k_{obs} = k_2[Br^-] + k_3[Br^-]^2 \quad (18)$$

Representative data are tabulated in Supporting Information, Table S4. At 298.0 K, $[H^+] = I = 0.1$ M, k_2 and k_3 are found to be (3.43 ± 0.26) × 10^{-2} M^{-1} s^{-1} and (4.82 ± 0.02) × 10^1 M^{-2} s^{-1}, respectively.

k_{obs} increases as the ionic strength decreases, as expected for a reaction between ions of opposite charge (Supporting Information, Table S5 and Figure S2).

The effects of acidity on the rate constants were studied at $[H^+] = 0.1 - 0.001$ M. Both k_2 and k_3 were found to increase with $[H^+]$. Plots of k_2 and k_3 versus $[H^+]$ are linear as shown in Figure 9. This is consistent with the relationship shown in eqs 19 and 20.

$$k_2 = k_{a2} + k_{b2}[H^+] \quad (19)$$

$$k_3 = k_{a3} + k_{b3}[H^+] \quad (20)$$

The overall rate law is shown in eq 21.

$$-\frac{d[Ru^{VI}]}{dt} = \{(k_{a2} + k_{b2}[H^+]) + (k_{a3} + k_{b3}[H^+])[Br^-]\}[Ru^{VI}][Br^-] \quad (21)$$

At 298.0 K and $I = 0.1$ M, $k_{a2} = (2.03 \pm 0.03) \times 10^{-2}$ M^{-1} s^{-1}, $k_{b2} = (1.50 \pm 0.07) \times 10^{-1}$ M^{-2} s^{-1}, $k_{a3} = (7.22 \pm 2.19) \times 10^{-1}$ M^{-2} s^{-1}, and $k_{b3} = (4.85 \pm 0.04) \times 10^2$ M^{-3} s^{-1}.

The activation parameters $\Delta H^‡$ and $\Delta S^‡$ were determined by studying the kinetics over a 30 °C temperature range. At $[H^+] = 0.07$ M and $I = 0.1$ M, $\Delta H^‡$ and $\Delta S^‡$ are (16.2 ± 1.2) kcal mol^{-1} and −(11 ± 4) cal mol^{-1} K^{-1}, respectively, for the k_2 path, (7.7 ± 0.7) kcal mol^{-1} and −(26 ± 2) cal mol^{-1} K^{-1}, respectively, for the k_3 path (Supporting Information, Figure S3).

The kinetics were carried out in D_2O at pD = 1.04, $I = 0.1$ M, and 298.0 K. $k_2(D_2O)$ and $k_3(D_2O)$ are (3.10 ± 1.08) × 10^{-2} M^{-1} s^{-1} and (6.42 ± 0.09) × 10^1 M^{-2} s^{-1} respectively (Supporting Information, Figure S4). The deuterium isotope effects are $k_2(H_2O)/k_2(D_2O) = 1.1 \pm 0.2$ and $k_3(H_2O)/k_3(D_2O) = 0.76 \pm 0.2$.

Mechanism. In the oxidation of Br^- by *trans*-$[Ru^{VI}(N_2O_2)(O)_2]^{2+}$ in aqueous solutions, parallel pathways that are first- and second-order in Br^- are observed, and both pathways are acid-catalyzed. Because the macrocyclic ligand N_2O_2 in *trans*-$[Ru^{VI}(N_2O_2)(O)_2]^{2+}$ is rather bulky, a second-order pathway that involves prior coordination of a Br^- to produce a seven-coordinate intermediate followed by oxidation of a second Br^- by this intermediate is rather unlikely. Also, as in the case of the oxidation of I^-, the dependence on $[H^+]$ probably does not arise from prior protonation of *trans*-$[Ru^{VI}(N_2O_2)(O)_2]^{2+}$.

There are two possible mechanisms for the oxidation of Br^-, namely, one-electron transfer and oxygen atom transfer, shown in eqs 22 and 23, respectively.

$$[Ru^{VI}(N_2O_2)(O)_2]^{2+} + Br^- \rightarrow [Ru^{V}(N_2O_2)(O)_2]^{+} + Br^{\bullet} \quad (22)$$

$$[Ru^{VI}(N_2O_2)(O)_2]^{2+} + Br^- + H^+ \rightarrow [Ru^{IV}(N_2O_2)(O)]^{2+} + HOBr \quad (23)$$

From the E^0 for the $Br^•/Br^-$ couple of 2.06 V[47] and the E^0 for $[Ru^{VI}(N_2O_2)(O)_2]^{2+}/[Ru^{V}(N_2O_2)(O)_2]^{+}$ couple of 0.94 V, ΔG^0 for the one-electron transfer pathway is 25.7 kcal mol^{-1}. This is much higher than the observed $\Delta G^‡$ value of 19.0 and 15.3 kcal mol^{-1} for the k_2 and k_3 pathways, respectively; hence, the electron transfer pathway can be ruled out.

On the other hand, a two-electron OAT step is expected to be only slightly uphill, as evidenced from the redox potentials shown in eqs 24[46] and 25.

$$HOBr + H^+ + 2e^- \overset{E^0 = 1.31V}{\rightleftharpoons} H_2O + Br^- \quad (24)$$

$$[Ru^{VI}(N_2O_2)(O)_2]^{2+} + 2H^+ + 2e^- \overset{E^0 = 1.22V}{\rightleftharpoons} [Ru^{IV}(N_2O_2)(O)(OH_2)]^{2+} \quad (25)$$

A proposed oxygen-atom transfer mechanism that is consistent with all the experimental observations is shown in eqs 26–33.

$$[O{=}Ru^{VI}{=}O]^{2+} + Br^- \overset{K_{OT}}{\rightleftharpoons} [O{=}Ru^{IV}{-}OBr]^+ \quad (26)$$

$$[O{=}Ru^{IV}{-}OBr]^+ + H_2O \xrightarrow{k_{27}} [O{=}Ru^{IV}{-}OH_2]^{2+} + OBr^- \quad (27)$$

$$[O{=}Ru^{IV}{-}OBr]^+ + H^+ + H_2O \xrightarrow{k_{28}} [O{=}Ru^{IV}{-}OH_2]^{2+} + HOBr \quad (28)$$

$$[O{=}Ru^{IV}{-}OBr]^+ + Br^- + H_2O \xrightarrow{k_{29}} [O{=}Ru^{IV}{-}OH]^+ + Br_2 + OH^- \quad (29)$$

$$[O{=}Ru^{IV}{-}OBr]^+ + H^+ + Br^- \xrightarrow{k_{30}} [O{=}Ru^{IV}{-}OH]^+ + Br_2 \quad (30)$$

$$[O{=}Ru^{IV}{-}OH]^+ + H^+ \rightarrow [O{=}Ru^{IV}{-}OH_2]^{2+} \quad (31)$$

$$OBr^- + H^+ \rightleftharpoons HOBr \quad (32)$$

$$Br^- + HOBr + H^+ \rightarrow Br_2 + H_2O \quad (33)$$

The initial step is reversible OAT from $O{=}Ru^{VI}{=}O$ to Br^- to generate $[Ru^{IV}(N_2O_2)(O)(OBr)]^+$. The latter species then undergoes parallel aquation (eqs 27 and 28) and oxidation of Br^- (eqs 29 and 30), both processes are acid-catalyzed. Aquation results in the formation of free HOBr which is known to rapidly oxidize Br^- to Br_2 with a rate constant of 2×10^{10} M^{-2} s^{-1}.[43] On the basis of the above scheme, the rate law is (for $K_{OT}[Br^-] \ll 1$)

$$-\frac{d[Ru^{VI}]}{dt} = K_{OT}\{(k_{27} + k_{28}[H^+]) + (k_{29} + k_{30}[H^+])[Br^-]\}[Ru^{VI}][Br^-] \quad (34)$$

This agrees with the experimental rate law shown in eq 21 with $K_{OT}k_{27} = k_{a2}$, $K_{OT}k_{28} = k_{b2}$, $K_{OT}k_{29} = k_{a3}$, $K_{OT}k_{30} = k_{b3}$.

Attempts to detect $HOBr/OBr^-$ by adding phenol red[25,48] to a 1:1 mixture of Ru^{VI} and Br^- were unsuccessful; no bromophenol blue was observed, presumably because the equilibrium concentration of $HOBr/OBr^-$ was very low.

Summary and Conclusion

In the oxidation of I^- by *trans*-$[Ru^{VI}(N_2O_2)(O)_2]^{2+}$, the results are consistent with parallel electron transfer and oxygen atom transfer pathways. On the other hand, in the oxidation of Br^-, which has a much higher $Br^{\bullet}/Br^-$ potential, OAT appears to be the only pathway. Both Br^- and I^- oxidations are acid-catalyzed; however, in the case of I^- the acid catalysis is proposed to occur in the ET and OAT steps, with the rate constant of the acid-dependent path 5 orders of magnitude faster than the acid-independent path. In the case of Br^- the acid catalysis appears to occur in reactions after the OAT step, with the acid-dependent rate constants 8 and 690 times faster than the acid-independent rate constants for the second-order and third-order pathways, respectively. Also, in the case of Br^-, the data are consistent with oxidation by both free and coordinated $HOBr/OBr^-$ ($pK_a = 8.59$),[49] whereas in the case of I^- it appears that oxidation by free HOI predominates (in the second phase), presumably because there is a larger steric effect for I^-.

Acknowledgment. The work described in this paper was supported by the Research Grants Council of Hong Kong (CityU 101403) and the City University of Hong Kong (9610020). We thank Mr. K. H. Chow for some initial experiments.

Supporting Information Available: Table of rate data and representative kinetic plots (PDF). This material is available free of charge via the Internet at http://pubs.acs.org.

IC8003849

(46) Mussini, T.; Longhi, P. In *Standard Potentials in Aqueous Solutions*; Bard, A. J., Parsons, R., Jordon, J., Eds.; Marcel Dekker: New York, 1985; pp 78−83.
(47) Woodruff, W. H.; Margerum, D. W. *Inorg. Chem.* **1973**, *12*, 962–964.
(48) Reynolds, M. S.; Morandi, S. J.; Raebiger, J. W.; Melican, S. P.; Smith, S. P. E. *Inorg. Chem.* **1994**, *33*, 4977–4984.
(49) Gerritsen, C. M.; Gazda, M.; Margerum, D. W. *Inorg. Chem.* **1993**, *32*, 5740–5748.